Turbulent Flows

Stephen B. Pope
Cambridge University Press, 2000

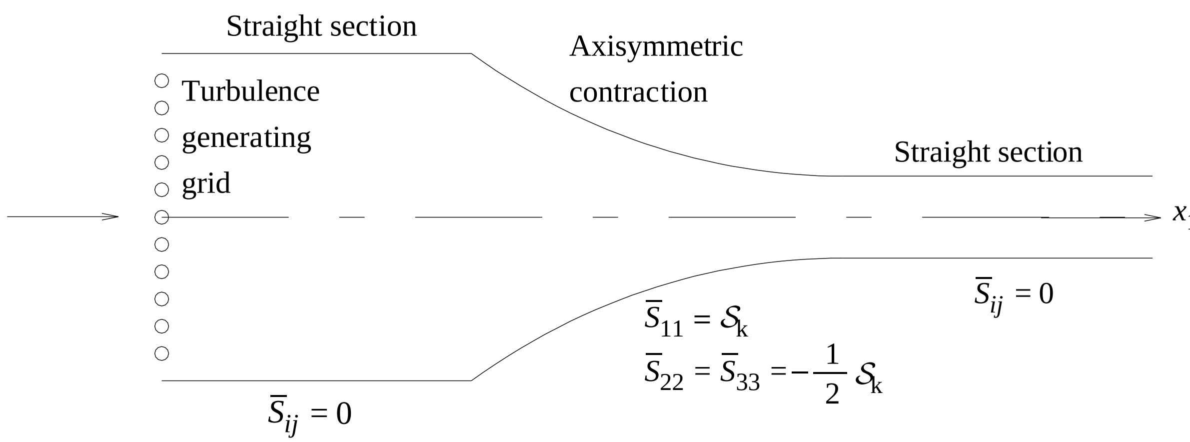

Figure 10.1: Sketch of an apparatus, similar to that used by Uberoi (1956) and Tucker (1970) to study the effect of axisymmetric mean straining on grid turbulence.

Turbulent Flows

Stephen B. Pope
Cambridge University Press, 2000

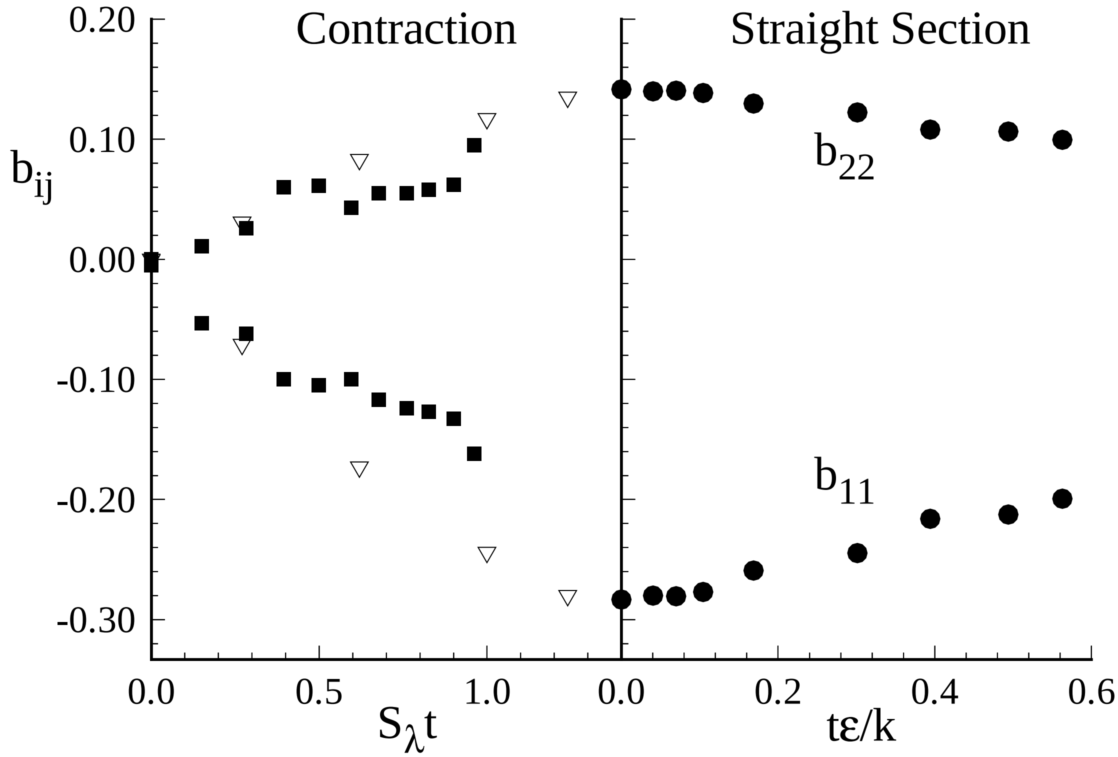

Figure 10.2: Reynolds-stress anisotropies during and after axisymmetric straining. Contraction: experimental data of Tucker (1970), $\mathcal{S}_\lambda k/\varepsilon = 2.1$; ∇ DNS data of Lee and Reynolds (1985), $\mathcal{S}_\lambda k/\varepsilon = 55.7$; flight time t from the beginning of the contraction is normalized by the mean strain rate $\mathcal{S}_\lambda$. Straight section: experimental data of Warhaft (1980); flight time from the beginning of the straight section is normalized by the turbulent timescale there.

Turbulent Flows

Stephen B. Pope
Cambridge University Press, 2000

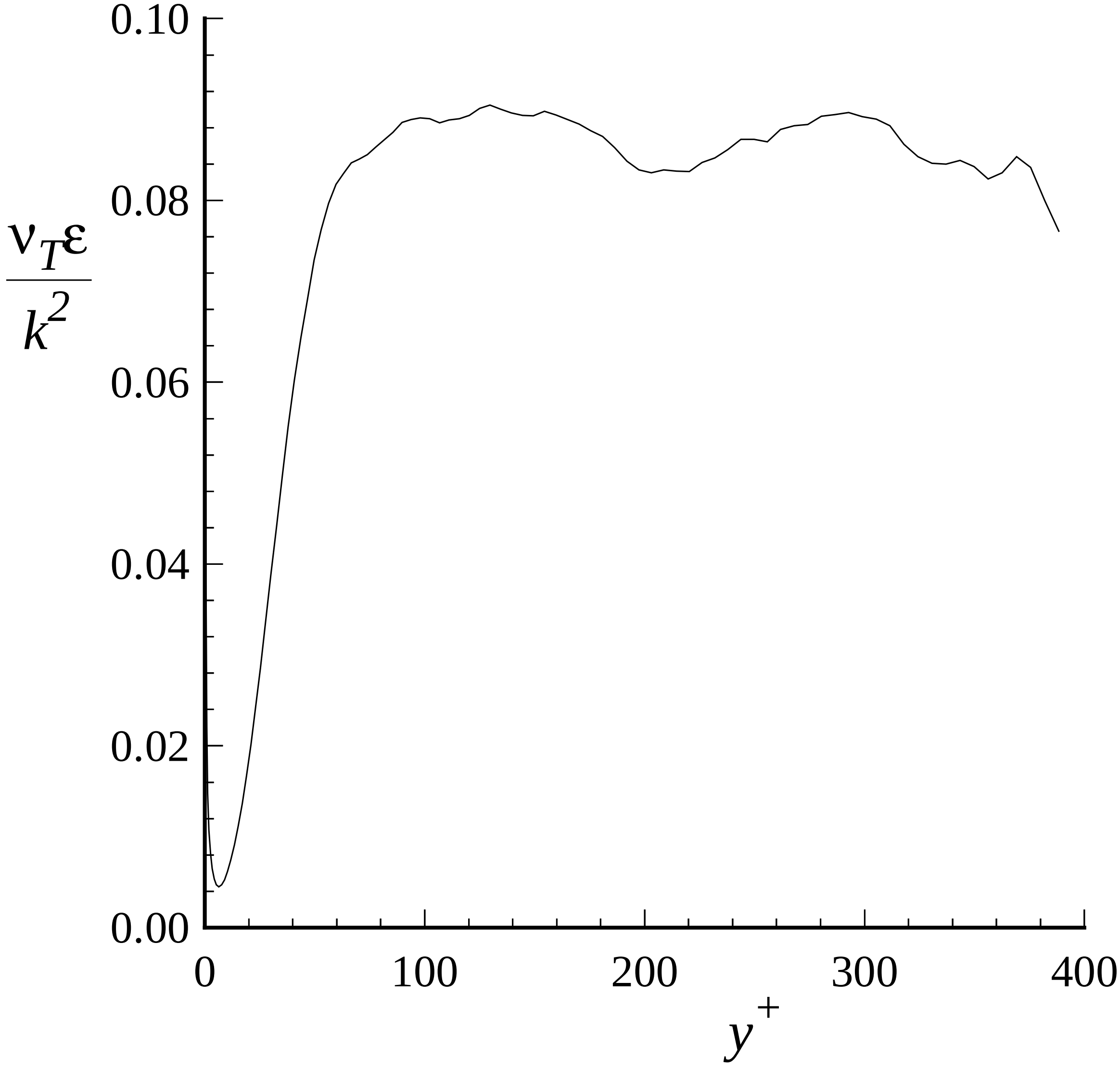

Figure 10.3: Profile of $\nu_T \varepsilon / k^2$ (see Eq. 10.39) from DNS of channel flow at Re$= 13,750$ (Kim *et al.* (1987)).

Turbulent Flows

Stephen B. Pope
Cambridge University Press, 2000

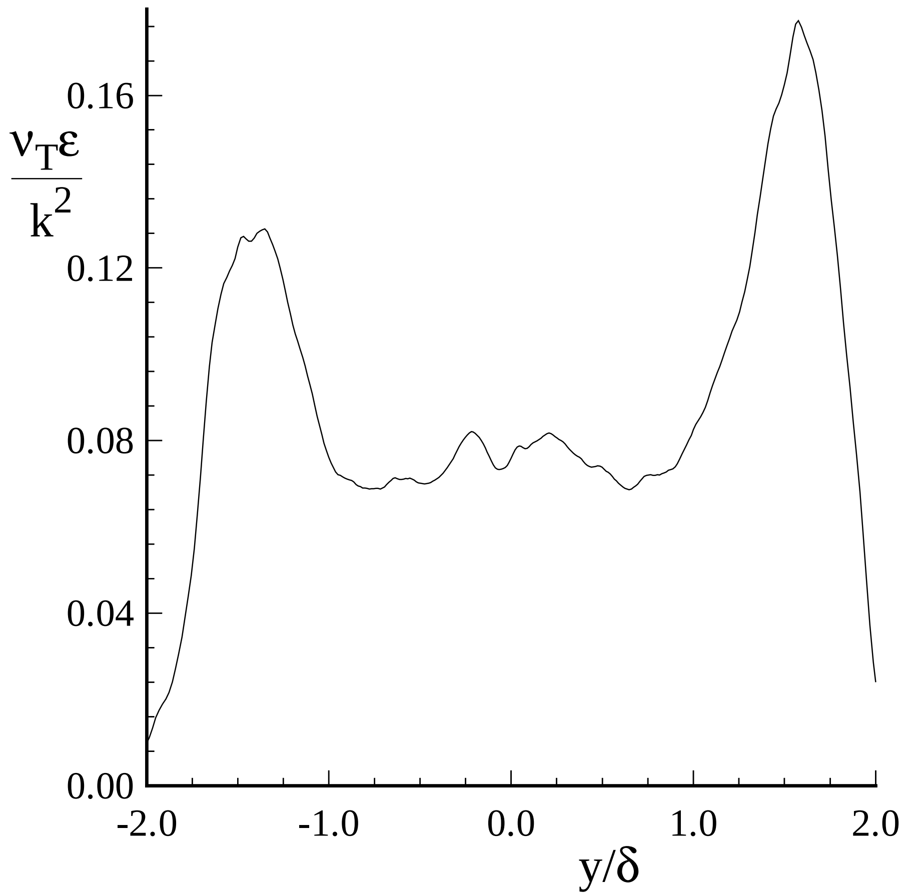

Figure 10.4: Profile of $\nu_T \varepsilon / k^2$ (see Eq. 10.39) from DNS of the temporal mixing layer (from data of Rogers and Moser 1994).